

Design and performance of a nanofiltration plant for the removal of chromium aimed at the production of safe potable water

Original

Design and performance of a nanofiltration plant for the removal of chromium aimed at the production of safe potable water / Giagnorio, Mattia; Steffenino, Sara; Meucci, Lorenza; Zanetti, Mariachiara; Tiraferri, Alberto. - In: JOURNAL OF ENVIRONMENTAL CHEMICAL ENGINEERING. - ISSN 2213-3437. - 6:4(2018), pp. 4467-4475.
[10.1016/j.jece.2018.06.055]

Availability:

This version is available at: 11583/2710823 since: 2018-07-13T11:19:22Z

Publisher:

Elsevier

Published

DOI:10.1016/j.jece.2018.06.055

Terms of use:

This article is made available under terms and conditions as specified in the corresponding bibliographic description in the repository

Publisher copyright

(Article begins on next page)

Design and Performance of a Nanofiltration Plant for the Removal of Chromium Aimed at the Production of Safe Potable Water

Mattia Giagnorio^a, Sara Steffenino^b, Lorenza Meucci^b, Maria Chiara Zanetti^a,

Alberto Tiraferri^{a,c*}

*^aDepartment of Environment, Land and Infrastructure Engineering (DIATI), Politecnico di Torino,
Corso Duca degli Abruzzi 24, 10129 Turin, Italy*

^bSMAT SpA, Società Metropolitana Acque Torino, Corso XI Febbraio 14, 10152 Turin. Italy

^cCleanWaterCenter@PoliTo, Politecnico di Torino, Corso Duca degli Abruzzi 24, Torino, Italy

* To whom correspondence should be addresses: Tel: +39-011-0907628; Fax: +39-011-0907699;

E-mail: alberto.tiraferri@polito.it

Abstract

Nanofiltration is an emerging technology applied to increase the availability of safe drinking water. This study evaluates nanofiltration as a feasible process to reach the new regulatory concentration limit for hexavalent chromium (0.01 mg/L) in potable water. Real well water contaminated with chromium was treated using two types of membranes of different selectivity in bench-scale and pilot-scale experiments. The pilot system comprised two modules in series and was run for 42 days without chemical cleaning, at an applied pressure of < 6 bar. A flux decline of around 20% of the initial value was observed with both membrane types. Observed rejection was constant (> 98%) for the denser membrane, while it decreased from 95% to 70% for the less selective membrane. This result may be attributed to the impairment of charge-based rejection of chromate ions. Based on these results, a full-scale plant is proposed to treat the contaminated well water, equipped with the more selective membranes. The optimal plant configuration would consist of two stages, with a total number of 96 modules to produce 30 L/s of potable water. Based on equations developed to describe contaminant concentrations in the streams entering and exiting a generic plant, guidelines are also provided to perform a preliminary system analysis. An economic assessment showed an average cost of <0.3 € per cubic meter of product water considering both capital and operational costs, for a plant lifetime of 10 years. From an environmental perspective, power supply would be the most impactful item of the plant.

Keywords

Nanofiltration; chromium; drinking water; pilot plant; techno-economic analysis; LCA.

1. Introduction

Membrane filtration systems are widely applied water treatment technologies, owing to their modular flexibility, limited space requirements, and lower amount of chemicals needed to run the process compared to other treatment techniques (Baker 2012). Specifically, nanofiltration (NF) has been increasingly investigated during the last decade. NF membranes remove multivalent ions and provide high water fluxes at relatively low applied pressures (Hilal et al. 2004). Various recent studies have investigated the practicability of NF as a wastewater and potable water treatment technology, a question that remains unanswered for several applications (Garcia-Ivars et al. 2017; Mohammad et al. 2015; Sarkar et al. 2007).

NF has been shown to be applicable to the removal of micropollutants from wastewater effluents (Luo et al. 2014), to the recovery of resources by treating wastewater from the textile industry (Lin et al. 2015), and to the improvement of the efficiency of advanced oxidation processes (Minella et al. 2018). A few pilot-scale studies have been performed to evaluate NF as an integral step of wastewater treatment, and investigations were carried out to analyse the performance of NF membranes in the presence of organic matter, dyes, and to treat complex waters (Bellona and Drewes 2007; Kurt et al. 2012; Ong et al. 2014; Wadekar et al. 2017). NF pilot plants showed promising results for contaminated groundwater treatment or for water recycling in the process industry (Bellona and Drewes 2007; Saitua et al. 2011). Pilot-scale experiments also addressed membrane fouling (Andrade et al. 2017; Chon and Cho 2016), which is regarded as the main bottleneck in NF applications.

As regards potable water production, NF may be applied for the removal of a wide range of organic and inorganic compounds, including pesticides and pharmaceuticals, from groundwater or surface water (Kosutic et al. 2004; Radjenovic et al. 2008; Sarkar et al. 2007; Taheran et al. 2016; Van der Bruggen and Vandecasteele 2003). It is also recognized as a valuable alternative to more conventional water softening systems (Bannoud 2001). However, the viability of NF as a

technology for drinking water production has not been tested experimentally at the pilot or field scale. Most of the available studies are based on theoretical analyses and comparisons between different water treatment systems, or on very specific pilot scale integrations (e.g., nanofiltration coupled with renewable energies or ultraviolet photolysis) (Garcia-Vaquero et al. 2014; Lopes et al. 2013; Vince et al. 2008). Moreover, the currently available economic assessments of NF systems for drinking water production are usually based on lab-scale experiments (Costa and de Pinho 2006).

NF has the potential of becoming a major technological solution for drinking water production as a result of the increasingly stringent legislative limits applied to ensure high water quality, hardly achievable with other more conventional treatment processes. This is the case of the new limit imposed for hexavalent chromium concentration in potable water (0.01 mg/L), which has recently come into force in Italy and in the UK (Council Directive 98/83/EC of 3 November 1998 1998; Guidelines for drinking-water quality 2011; Legislative Decree 2 February 2001, n. 31 2016). NF is certainly one of the most promising available technologies for the removal of metal ions from aqueous solutions (Al-Rashdi et al. 2013; Mikulasek and Cuhorka 2016). In particular, in a recent paper (Giagnorio et al. 2018), we have demonstrated the possibility to efficiently reduce the concentration of chromium present in contaminated waters below the new threshold value of 0.01 mg/L by using different commercial NF membranes. Through laboratory experiments, we have shown the influence of different parameters (e.g., solution chemistry and membrane properties) on filtration process performance.

The aim of this study is to evaluate and discuss the feasibility of a nanofiltration plant for the purification of chromium-contaminated waters for drinking water production. The discussion (i) assesses the feasibility of a full-scale plant that would treat real well water and (ii) provides design guidance for the implementation of similar NF plants. We present the results obtained with two commercial nanofiltration membranes with different intrinsic selectivity. Following preliminary

laboratory experiments, field tests are discussed with a NF pilot plant comprising two membrane modules in series and installed to work continuously to purify the polluted well water. The performance of the pilot plant is evaluated and a techno-economic and environmental assessment of a potential full-scale NF plant is discussed. Additionally, a system-scale analysis is presented that may be readily applied for a preliminary computation of the main design parameters of an NF plant treating a wide range of waters.

2. Materials and Methods

2.1 Well water characteristics

Table 1 reports the characteristics of the well water in the investigated site near Turin, Italy. Before the new legislative limit came into force, an average flow rate of 30 L/s drinking water was delivered from this source to provide water to roughly 13000 residents. The water was delivered after a mild disinfection step. Due to the presence of hexavalent chromium at a medium-high concentration of 0.023 $\mu\text{g/L}$, the discussed well water no longer meets the latest legal restrictions. The water has high hardness and a total ionic strength of 14.3 mM.

Table 1: Well water characteristics

pH	7.5
Conductivity ($\mu\text{S}/\text{cm}$)	646
Hardness ($^{\circ}\text{F}$)	36.8
HCO_3^- (mg/L)	363
Alkalinity (meq/L)	7.24
Aggressive Index	12.6
Ionic Strength	14.3
Cl^- (mg/L)	9.9
F^- (mg/L)	0.11
PO_4^{3-} (mg/L)	0.03
NO_3^- (mg/L)	7.9
SO_4^{2-} (mg/L)	34
Ca^{2+} (mg/L)	110
Mg^{2+} (mg/L)	23
K^+ (mg/L)	1
Na^+ (mg/L)	11
As ($\mu\text{g}/\text{L}$)	1
B ($\mu\text{g}/\text{L}$)	32
Co ($\mu\text{g}/\text{L}$)	59
Cr ($\mu\text{g}/\text{L}$)	23
Fe ($\mu\text{g}/\text{L}$)	32
Mn ($\mu\text{g}/\text{L}$)	13
Cu ($\mu\text{g}/\text{L}$)	0.12
Se ($\mu\text{g}/\text{L}$)	2.2
Zn ($\mu\text{g}/\text{L}$)	15

2.2 Membranes

Two different commercial NF membranes were studied: NF270 and NF90 (Dow Chemical Company, Midland MI). These membranes are composite and consist of a semi-aromatic polyamide layer cast on top of a polysulfone microporous support. Non-woven polyester fabric is used as a mechanical substrate for both membranes. Membrane transport characterization and the main membrane parameters are reported in Table 2 (Giagnorio et al. 2018). Zeta potential measurements showed a negatively charged surface under neutral pH conditions for both membranes. NF90 is more selective and less permeable than NF270.

Table 2: Characteristics of the membranes used in this study

Membrane	Water Permeance (LMH/bar)	MgSO ₄ rejection (%)	NaCl rejection (%)	Roughness (nm)	Active layer thickness (nm)	Zeta Potential (mV) ^a
NF270	18.8	98.8	> 99.5	4.2 ± 0.3 (Semiao and Schafer 2013)	21 ± 2.4 (Semiao and Schafer 2013)	-23
NF90	6.9	98	52 (Semiao and Schafer 2013)	61.7 ± 2.1 (Semiao and Schafer 2013)	218 ± 40 (Semiao and Schafer 2013)	-17

^a Measured at pH 7.4 in 10 mM NaCl

2.3 Laboratory nanofiltration setup and test protocol

The filtration unit comprises: high-pressure pump (Hydra-cell pump, Wanner Engineering, Inc., Minneapolis, MN), feed vessel, flat membrane housing cell, temperature control, and data acquisition system. The housing cell consists of a 7.9 cm long, 2.9 cm wide, and 0.3 cm high rectangular channel. The active area of the membrane sample is 23 cm². The permeate flow rate was automatically measured every 60 seconds using a computer-interfaced balance. A detailed description of the cross-flow lab-scale system is reported in our previous publication (Giagnorio et al. 2018).

Lab experiments were performed filtering well water with both NF270 and NF90 membranes. Prior to each experiment, the membrane samples were compacted for 14 h at 150 psi (10.3 bar). Tests were then performed with a constant applied pressure of 100 psi (6.9 bar), a cross-flow velocity of 4.5 L/min, and an average feed solution temperature of 22 °C. Both the permeate and the concentrate streams were recirculated back into the feed tank. Feed and permeate samples were analysed by an external accredited company (Eurolab S.r.l., Italy) to fully characterize the anion/cation concentration in solution, as well as the content of metals and organic matter.

2.4 Nanofiltration pilot plant and field experiments

A schematic diagram of the nanofiltration pilot plant is presented in Figure 1; a picture of it is available in the Supplementary Material file (Figure S1). A hydraulic pump was used to feed well water to the system. A stainless-steel housing was used to accommodate two spiral-wound membrane modules in series. The applied pressure was controlled by the upstream valve and by the concentrate valve. A digital manometer measured the pressure at the inlet of the housing while two flow meters measured concentrate and permeate flow rates. The system was run with an inlet flow rate of 2000 L/h, a cross-flow rate of 26.7 L/min, and a total recovery rate of 20%. Full-fit fiberglass 4040 spiral wound elements were used for both NF270 and NF90 membranes. The dimensional characteristics of the 4040 module are reported in Table 3, together with its operating limits determined from (i) the design guidelines reported by the manufacturer and (ii) the quality of the feed water (i.e., a silt density index, SDI, < 3)

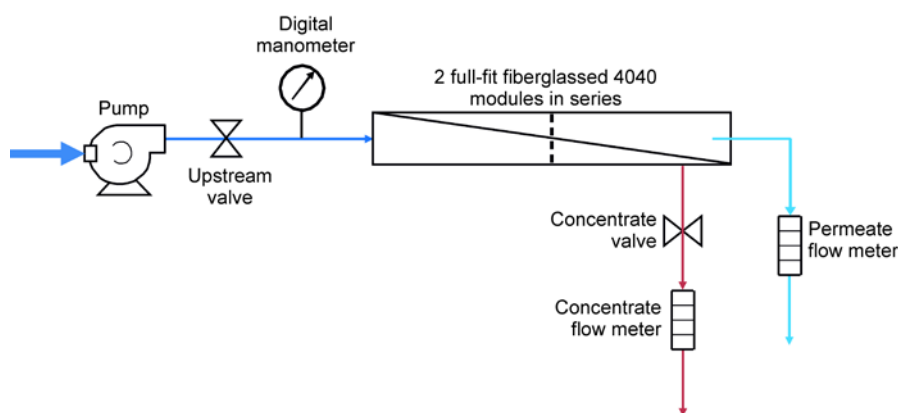


Figure 1: Schematic representation of the nanofiltration pilot plant. The plant was designed to work with two NF-4040 modules in series.

Table 3: Dimensional characteristics and operating limits of the NF-4040 spiral-wound modules

Active Area (m ²)	7.6
Length (m)	1.016
Diameter (cm)	99
Maximum Operating Pressure (bar)	41
Maximum Feed Flow Rate (m ³ /h)	3.6
Maximum Permeate Flow Rate (m ³ /h)	0.325
Minimum Concentrate Flow Rate (m ³ /h)	1.4
Maximum element recovery (%)	19

Two different pilot scale tests were performed: the first with NF270 modules and the second with NF90 modules. For each test, the pilot plant was run for 42 days, keeping a constant applied pressure of 5.25 (76 psi) for NF270, and 5.75 bar (84 psi) for NF90, respectively, at the inlet of the housing. The well water described in Table 1 was not subjected to any pre-treatment. The changes in permeate and concentrate flow rates were recorded over time. To measure chromium concentration, permeate and feed water samples were collected twice per week. The analyses were performed with an inductively coupled plasma optical emission spectrometry by SMAT S.p.A, the water utility company owner of the water well. A mild physical cleaning of the modules was performed by increasing the cross-flow velocity to 30 L/min for 1 hour every week. The system did not undergo any chemical cleaning during the testing periods.

3. Plant design, system scale modeling, and LCA

3.1 Plant design and system-scale modeling

Two software programs were used to design the full-scale nanofiltration plant and to assess the quality of the treated water. WAVE (Dow Water & Process Solutions) was employed to evaluate the best module configuration and to simulate the chemical composition of the treated water. AQION was used to calculate the hydrochemistry and to quantify the Aggressive Index (A.I.) of the water streams.

A system-scale analysis was developed to generalize the system design and to evaluate the main design parameters of a membrane plant in terms of pollutant concentration: (i) c_F , concentration of pollutant in the feed solution entering the system (Feed); (ii) c_C , concentration of pollutant in the concentrate leaving the system (Concentrate); (iii) c_{TW} , concentration of pollutant in the treated water (Permeate); (iv) REC , recovery rate, i.e., the ratio between the flow rate of the treated water and that of feed water; (v) Rej , the observed system rejection, defined as $Rej = \left(1 - \frac{c_{TW}}{c_F}\right)$. For this analysis, the membrane system was modeled by discretizing the control volume from the inlet of the feed stream to the outlet of the concentrate stream. REC may be regarded as the variable describing the temporal or spatial scale of the system from the inlet to the outlet. This simulation was carried out for a number of Rej values, thus simulating the performance that would be obtained by applying membranes with different transport characteristics. A semi-empirical approach was adopted to derive the system equations. First, calculations were performed by fixing the value of one of the concentration parameters and finding the trend relating the other two concentration parameters as a function of REC for any given value of Rej . The concentration parameters were varied discretely across a wide value range. The best analytical expressions were then derived, by fitting the results obtained for the control volume:

$$c_C = c_F e^{A \cdot Rej} \quad (1)$$

$$c_{TW} = c_F \left[\frac{1}{REC} - \left(\frac{1}{REC} - 1 \right) e^{A \cdot Rej} \right] \quad (2)$$

$$\text{where: } A = \infty - \frac{\infty}{(1 - REC)^{\frac{1}{\infty - 1}}} \quad (3)$$

The term A needs to be calculated by finding the limit of equation 3 for a certain value of REC . Therefore, the redundant equation relating c_{TW} to c_C is:

$$c_{TW} = c_C \left[-\left(\frac{1}{REC} - 1 \right) + \frac{1}{REC} e^{-A \cdot Rej} \right] \quad (4)$$

This analysis is valid for a system comprising: one stage only, i.e., the concentrate stream does not undergo further filtration; one pass only, i.e., the permeate stream does not undergo further filtration; and no bypass, i.e., 100% of the feed water is treated. This analysis is independent of the number of vessels or modules, but it implicitly assumes that all vessels contain the same number of modules in series. Equations 1-4 derived in this study may be applied to conduct a preliminary estimation of the value of one of the concentration parameters according to the known or imposed value of the other parameters. For example, it would be possible to estimate the concentrations of a pollutant in a final product water obtained by treating feed water with a given level of contamination, using a specific membrane, i.e., a given value of observed rejection, and by simulating systems characterized by different recovery rates.

3.2 Life Cycle Assessment

A life cycle assessment of the full-scale NF plant was performed with the OpenLCA software. OpenLCA LCIA methods 1.5.7, with the ReCiPe methodology, was used as impact assessment method. Both midpoint and endpoint indicators were considered, the latter presented as normalized values with respect to the total computed endpoint impact. To evaluate the environmental burdens of the full-scale NF plant, the average daily drinking water demand of the specific location (30 L/s) was considered as functional unit. Attributional LCA with a hierarchist (H) perspective was selected. The inventory data for the NF system were calculated based on the available literature (Bonton et al. 2012), while the concentrate disposal and the energy requirements were directly imported from the analysis carried out through WAVE. The decommissioning of the NF system was not taken into account in the LCA analysis, due to the results presented in a previous paper (Bonton et al. 2012), which showed negligible burdens related to the disposal of building construction of similar membrane plants.

4. Results and Discussion

4.1 Membrane performance with real well water

Figure 2 depicts the rejection of different inorganic compounds present in the well water observed in lab experiments deploying NF270 and NF90 membranes. As expected, NF90 had higher removal rates than NF270, with a rejection above 80% for most of the elements or ions. Consistent with literature reports, boron was the only element removed at low rate (Hilal et al. 2011; Richards et al. 2010). Nanofiltration membranes cannot achieve significant rejection of boron at neutral pH, due to the predominance of its uncharged aqueous species, i.e., boric acid. Multivalent anions, together with cobalt, iron, manganese, and selenium were almost completely rejected by both membranes. Zinc removal was, instead, strongly dependent on the nature of the associated ions, as already reported in previous studies (Ben Frares et al. 2005). NF270 membranes showed lower rejection for all cationic elements in solution, being charge exclusion their main separation mechanism (Giagnorio et al. 2018). Conversely, NF90 membranes also separate compounds through size-dependent mechanisms (Giagnorio et al. 2018). These results suggest the feasibility of reducing the concentration of chromium in potable water with both membranes. The divalent chromate anion CrO_4^{2-} is the predominant chromium species in drinking water and may be removed through a combination of electrostatic repulsion exerted by the negatively-charged membrane surface and size-exclusion mechanisms (Giagnorio et al. 2018). Specifically, NF270 and NF90 samples had a chromium removal of 78 and 98%, respectively. Fluoride, chloride, and nitrate have little charge density and are mainly removed by size exclusion, which is consistent with our results showing significantly higher rejection with NF90 compared to NF270. Epsztein et al. have reported a full study on monovalent anion removal through nanofiltration, showing the fundamental role of Donnan exclusion and the possible influence of other compounds present in solution (Epsztein et al. 2018). The concentrations of the other elements or ions in the permeate stream were also well below the limits imposed by the Italian legislation (see Supplementary Material Table S1). In terms

of water flux, the looser NF270 membrane displayed only slightly greater values ($40.3 \text{ L m}^{-2}\text{h}^{-1}$) than the tighter NF90 membrane ($37.5 \text{ L m}^{-2}\text{h}^{-1}$) at equivalent applied pressure.

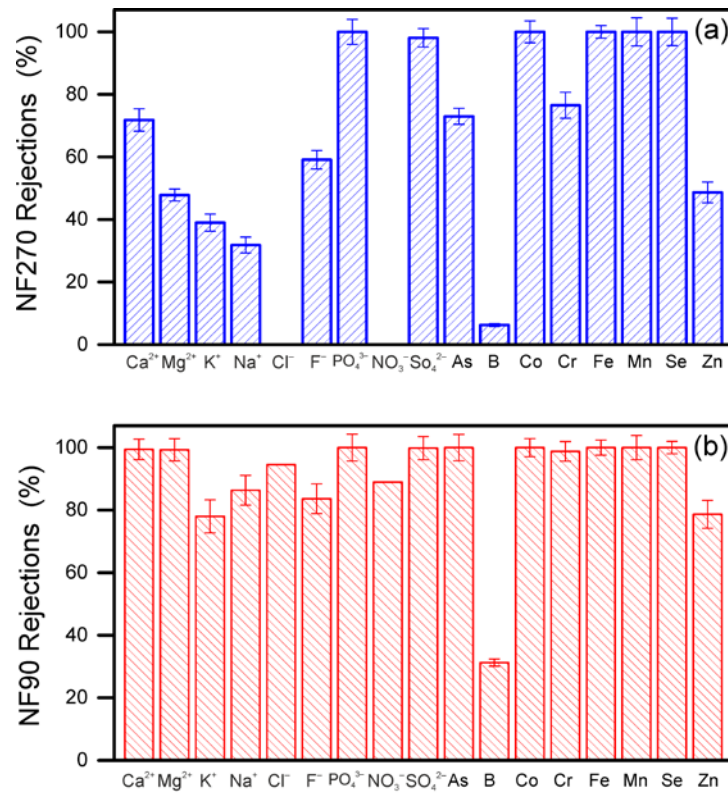


Figure 2: Rejection of the most common cations, anions, and metals from the well water described in Table 1 for a) NF270 and b) NF90 membranes.

4.2 Performance of the nanofiltration pilot plant

To validate the results obtained in laboratory tests and evaluate NF as a feasible drinking water production technology for waters contaminated with chromium, two field experiments were performed with the NF pilot plant schematically depicted in Figure 1. The results of both tests are presented in Figure 3. The tests started with a flux of treated water of roughly 480 L/h. Flow rates obtained in the lab were 480 L/h and 475 L/h with NF270 and NF90, respectively, consistent with pilot scale measurements at the beginning of the field tests. During the 42 day experiment, both membranes showed significant flux decline, likely due to organic fouling and to the precipitation of metals and carbonate species onto the membrane surface. This is in accordance with previous studies that evaluated fouling and scaling on the membrane surface with similar feed waters

(Espinasse et al. 2012; Vrijenhoek et al. 2001). The decline was slightly more pronounced for the NF90 modules, due to their higher selectivity and larger operating pressure compared to the NF270 membranes. The tests were conducted without chemical cleaning but with a very mild physical cleaning of the membranes, which consisted in running the feed water at a higher flow rate for 1 hour per week. The flux trends presented here represent the worst possible scenario, i.e., the most conservative case, for such a system. Therefore, flux decline would be significantly lower during real application and with proper management of the system.

Figure 3b and 3c show chromium rejection and chromium concentration values in the treated water, respectively. The more selective NF90 membranes maintained a constant observed Cr rejection of roughly 98% throughout the test, with a resulting Cr concentration in the treated water invariably smaller than 0.5 µg/L. NF270 membranes, on the other hand, were characterized by a gradual decrease of Cr rejection from 95% to 70% during the 42 days of operation. We attribute this to the influence of fouling, scaling, and fouling-enhanced concentration polarization on membrane performance. These phenomena result in the neutralization and/or shielding of the negative surface charges of the membrane, which lower its ability to reject chromium anions (CrO_4^{2-}) - the major chromium species in natural waters - by charge exclusion effects. Conversely, a reduction of the surface negative electric potential hardly affects size-based rejection mechanisms, which is consistent with the high removal rate exhibited by NF90 modules.

The lab experiments discussed above showed an average chromium rejection of 98.8% and 76.5%, for the NF270 and the NF90 membrane samples, respectively. Overall, it can be stated that both fluxes and rejection rates observed in laboratory experiments were consistent with those observed in the pilot tests. In particular, the permeate flux obtained in the lab may be regarded as the initial permeate flux for field applications, or the flux that would be observed in real applications employing clean membranes. As concerns chromium removal, the rejection values measured in the lab were representative of the values observed during the pilot tests once steady-

state conditions were reached. These results suggest that laboratory experiments are to a significant degree representative of field application of membranes, a conclusion that is not necessarily obvious given the different scales involved.

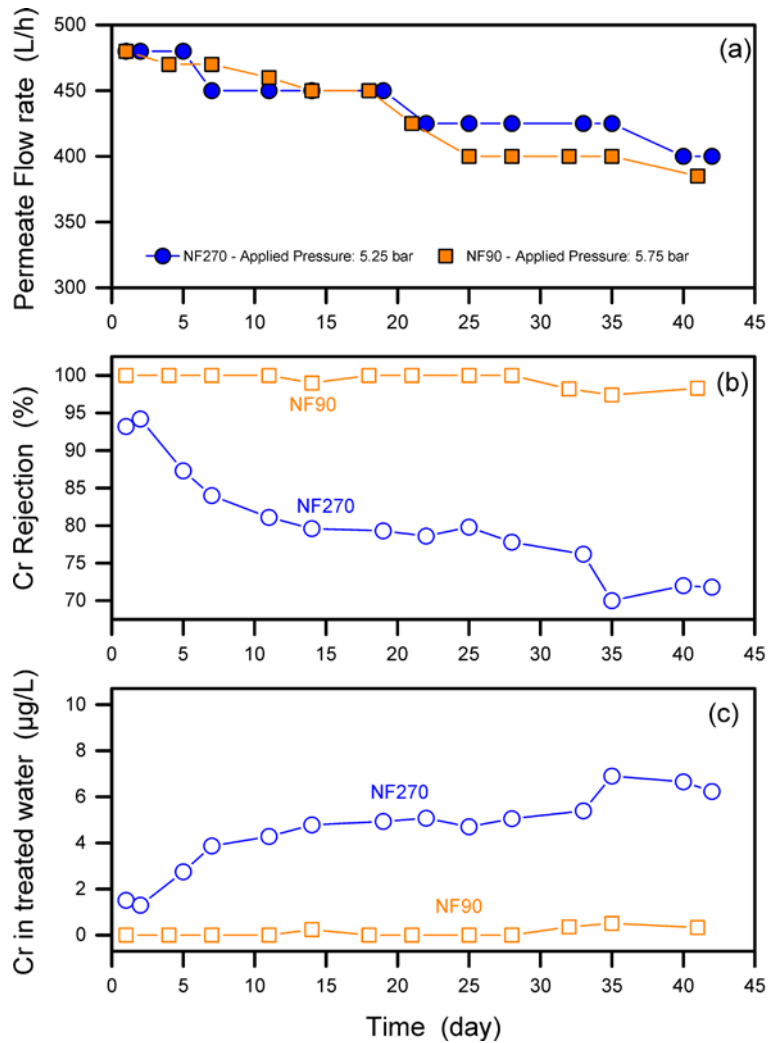


Figure 3: Performance of the nanofiltration pilot plant. a) Permeate flow rate, b) Total chromium observed rejection, and c) Chromium concentration measured in the treated water. Results are presented for NF270 (blue circles) and NF90 (orange squares) for a test period of 42 days. Each data point refers to an individual sample and measurement. Lines are only intended as guide for the eyes.

4.3 Design of the full-scale nanofiltration plant

Given the promising results obtained from the pilot tests, especially those testing the application of NF90 membranes, a full-scale NF plant was designed for the specific water source investigated in this study. The proposed configuration is site-specific; however, this calculation provides an indication of the overall system needs, performance, and cost of plants of similar size, i.e., feed flow rate of tens of L/s. Also, this design gives an insight on the overall feasibility of the application of nanofiltration for the removal of chromium and of heavy metals in general.

The design simulation was performed taking into account (i) the drinking water demand of the specific location (30 L/s of potable water must be delivered to the surrounding area) and (ii) a value of 80% for the recovery of the filtration unit. Based on the results obtained for the chromium removal by the field experiments, the membrane system was designed to work with NF90 membrane modules. Specifically, NF90-400/34i modules were adopted, characterized by an active area of 37.2 m² per module. The dimensional characteristics and the operating limits of this module type are reported in the Supplementary Material, Table S2.

Figure 4 shows a schematic representation of the best configuration designed for the NF plant. Well water is pumped to Stage 1, which is operated with nine vessels, and the concentrate from this stage is then processed by Stage 2, comprising six vessels. The total permeate produced is collected and mixed with a fixed percentage of bypassed well water, while the concentrate is disposed of in the sewage system. The function of the bypass is to reduce the total flow rate that needs treatment, which in turn allows a reduction of the plant size, and ensures that the final drinking water is indeed potable and contains an appropriate mixture of ions. In particular, the membrane configuration described in Figure 4 would allow a range of bypass values between 0% and 30%.

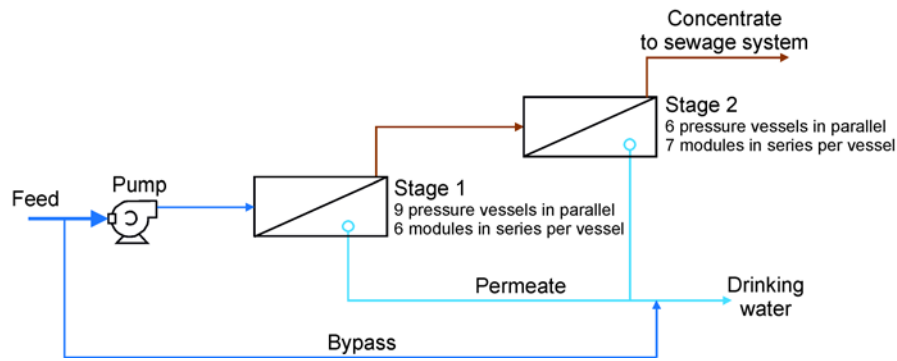


Figure 4: Design of the nanofiltration pilot plant. Two stages are included. Stage 1 designed with 9 pressure vessels and 6 modules per vessel. Stage 2 designed with 6 pressure vessels and 7 modules per vessel.

The results of the simulation of the full-scale design in Figure 4 are reported in Figure 5a. Here, chromium concentration and the aggressive index of the final product water are plotted as a function of percentage of bypass. Clearly, chromium concentration increases as a lower proportion of the feed water is filtered. Also, the A.I. increases as a lower proportion of demineralized water is mixed with the feed water to achieve a final water product. Aiming for a safety value of $5 \mu\text{g/L}$, i.e., the maximum chromium concentration in the product water, and for a minimum A.I. of 10, the suitable configurations for the NF system would be characterized by a bypass in the range 10-15%. Below this range, the product water would be too aggressive, while above these values it would contain a concentration of Cr too close to the limit of $10 \mu\text{g/L}$.

Figure 5b-d shows the results obtained by applying equation 1-4 to perform a system analysis. This analysis was conducted for typical concentration ranges of toxic metals and specifically for relevant concentrations of chromium in groundwaters. Figure 5b is a contour plot of the computed chromium concentration in the concentrate stream as a function of Cr concentration in the feed stream and of recovery rate, at a specific observed system rejection of 98% (i.e., the Cr removal rate of the NF90 membranes). Feed Cr concentration and recovery are represented on a linear scale on the left vertical and bottom horizontal axes, respectively. Dotted lines are drawn in the graph to

exemplify the case of the NF plant designed for the specific location considered in this study. This graph can be used to estimate the largest possible recovery resulting in Cr concentration in the retentate that meets the limits for the disposal of this stream in the sewage system. In our case, having 23 $\mu\text{g Cr/L}$ in the well water and a recovery rate of 80%, the concentrate would contain about 100 $\mu\text{g/L}$ of Cr. This value is below the legislative limit for the disposal of this stream in the sewage system as ruled by the Italian law, i.e., 200 $\mu\text{g/L}$.

A more detailed analysis is reported in figure 5c, always for a specific value of observed rejection of 98%. This graph shows the boundaries of the highest applicable recovery rates above which the concentration of Cr would exceed 5 $\mu\text{g/L}$ in the treated water and 200 $\mu\text{g/L}$ in the concentrate stream. The results suggest that the most relevant design parameter, when using NF90 membranes, is the concentration of Cr in the retentate, as this boundary (blue line connecting squares) sits below that related to the permeate concentration (red line connecting circles). This means that designing a plant with higher recovery would guarantee the safety of the treated water but prevent low cost disposal of the concentrate in the sewage system. This conclusion is true for high selectivity membranes; with decreasing rejection capabilities, the two boundaries first overlap and then cross each other, with the permeate value becoming the governing design parameter; please refer to the Supplementary Material (Figures S2-4) for similar analyses performed with lower observed system rejections of 75, 85, 90, or 95%. Finally, figure 5d presents another possible output of the system analysis, where Cr concentration in both the retentate stream (left axis) and treated water (right axis) is plotted as a function of recovery rate for four specific Cr concentrations in the feed solution. While these graphs were obtained for specific concentration ranges relevant for the present study, they can be extended to wider concentration ranges and simply represent examples of how equation 1-4 may be used to obtain useful first-hand data on system performance.

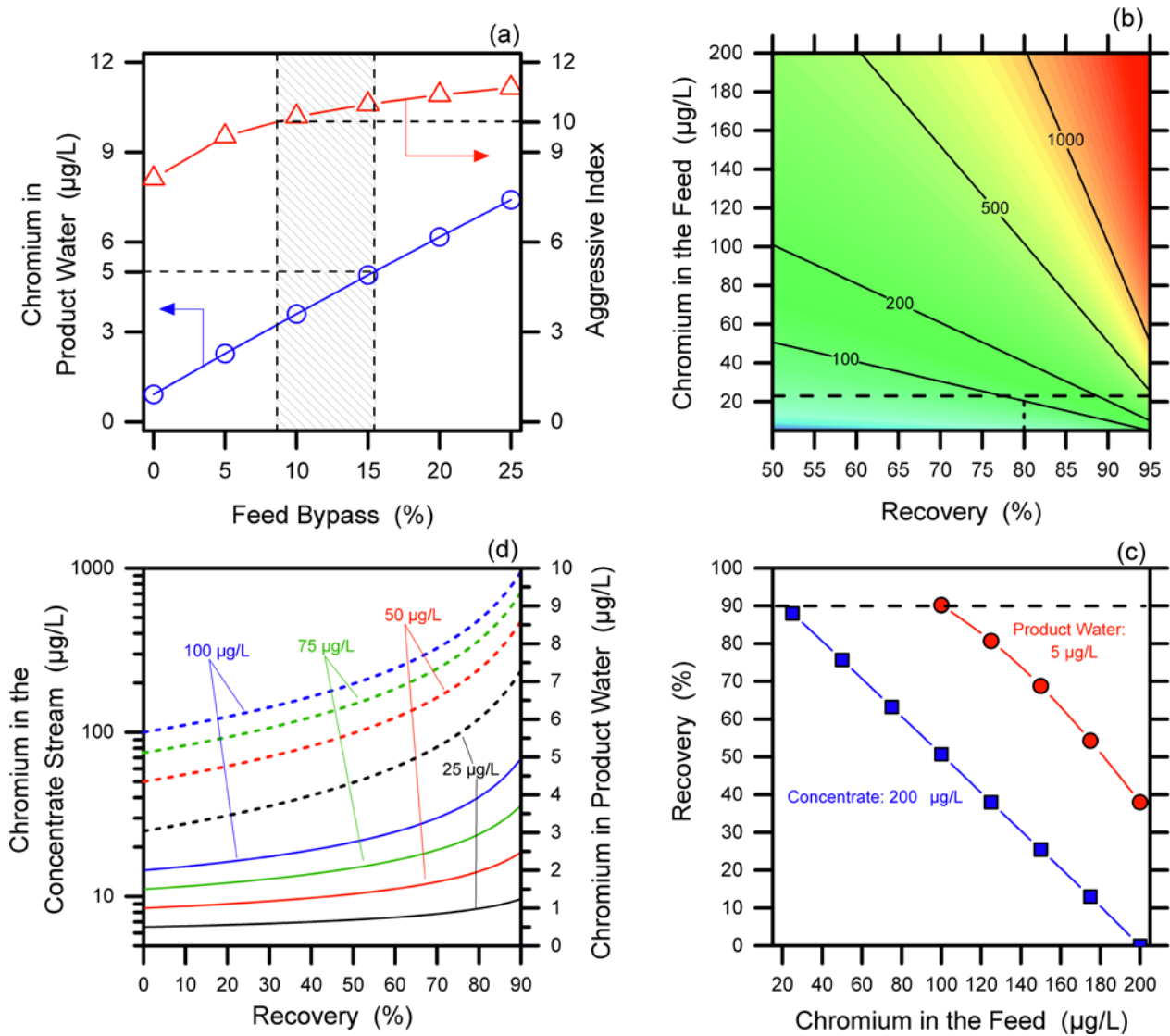


Figure 5: Results of the system modeling and performance of the NF full-scale plant. a) Chromium concentration and aggressive index of the product water, as a function of the percentage of feed bypass, for the full-scale NF configuration of Figure 4 using NF90 modules. b) Chromium concentration in the concentrate stream as a function of recovery rate and Cr concentration in the feed stream, at a system rejection of 98%. c) Maximum recovery rate as a function Cr concentration in the feed stream to obtain a Cr concentration in the treated water of 5 $\mu\text{g/L}$ (red circles) and a Cr concentration in the concentrate stream of 200 $\mu\text{g/L}$ (blue squares), for a system rejection of 98%. d) Chromium concentrations in the product water and in the concentrate stream as a function of the recovery rate for four values of Cr concentration in the feed water for a system rejection of 98%.

4.4 Economic assessment

An economic assessment of the full scale nanofiltration plant is reported in Figure 4. The capital cost of plant installation was estimated based on the data presented by Samhaber *et al.*, which summarize the installation and equipment costs of NF plants as a function of the volume of product water (Samhaber and Nguyen 2014). In particular, an exponential decrease of the specific equipment cost (SEC) was estimated with the increase in total active area of the plant, reaching a plateau with an average cost of roughly 360 €/m² for plants designed to work with membrane areas larger than 500 m². A membrane replacement cost of 0.017 € per m³ of product water was estimated based on a membrane lifetime of 5 years and a cost of about 800 € for each membrane module. Schafer *et al.* have estimated a similar cost for NF membranes applied to remove organic matter from water (Schafer et al. 2001). Based on the selected geographical region, an average cost of 0.15 €/kWh⁻¹ was considered for the energy requirements, and 0.31 €/m⁻³ for concentrate disposal in the sewage system (Water Management Tariffs 2018). As reported in the literature, the total cost of chemical reagents for membrane cleaning was estimated as 0.01 € for each m³ of water produced, taking into account the chemicals suggested by the membrane manufacturing for conventional cleaning-in-process operations (Costa and de Pinho 2006; Minella et al. 2018).

Table 4 presents the computed capital and operating costs, together with a summary of the operating parameters for the NF plant. Overall, the plant was designed to supply 2593 m³/day of drinking water with 96 NF90-400/34i membrane modules, for a total membrane area of 3568 m². The calculations were performed based on an ideal recovery rate of 80% and a feed bypass of 12.5%. Based on the results presented in Figure 5a, this configuration would allow the abatement of chromium below 4.3 µg/L, keeping an overall A.I. of the product water above 10. The concentrated stream results in a Cr concentration of 112 µg/L, well within the limits for disposal into the wastewater system. The plant installation cost was estimated around 1.3 million euro and a total daily cost of 586 € was calculated considering (i) a lifetime of 10 years for the membrane

filtration plant and (ii) the amount of water to be produced per day. It can be observed that the economic assessment of the NF plant is strongly influenced by energy and concentrate disposal costs, which amount to 17 % and 24 % of the total daily cost, respectively. Also according to previous studies, the costs related to membrane replacement and chemicals are not significant compared to the first two discussed operational costs (Costa and de Pinho 2006; Minella et al. 2018). Therefore, improvement of specific cleaning procedures may not be crucial for economic saving. On the other hand, coupling the NF system with renewable energy sources would result in overall economic benefits.

Table 4: Economic assessment of the nanofiltration plant designed

Operating parameters	
Drinking water supply (m ³ /day)	2593
Total well water (m ³ /day)	3142
Bypass water (m ³ /day)	393
Feed water to NF (m ³ /day)	2749
Permeate water produced (m ³ /day)	2200
Concentrate water produced (m ³ /day)	549
Cr concentration in the product water (µg/L)	4.26
Cr concentration in the concentrate stream (µg/L)	112
Aggressive index of produce water	10.4
Total membrane area (m ²)	3568
Feed Pressure (bar)	6.56
Specific energy (kWh/m ³ of pumped water)	0.29
Total installation cost of the plant (€)	1,296,000
Cost per m³ of portable water provided (€)	
Capital costs (depreciation, lifetime 10 years)	0.14
Energy	0.046
Concentrate disposal	0.066
Chemicals	0.009
Membrane replacement	0.01
TOTAL	0.271

The main alternative technology for the removal of chromium from potable water is based on ion-exchange resins. Specifically, Amberlite PWA7 produced by Dow Chemical is used to treat

well water in a location close to the site studied in this paper. A volume of 400 L of non-regenerative Cr selective resin is currently employed to treat 0.8 L/s well water with characteristics similar to those reported in Table 1, with the exception of a lower chromium concentration (i.e., 15 $\mu\text{g/L}$). Based on the available data, the adsorption limit is estimated at approximately 200 mg of chromium per liter of resin, at which point the value of 5 μL of Cr is reached in the product water. At that point, the resins cannot be regenerated and must be replaced. Based on these data, we estimated the volume of the same type of resin that would be needed in the location considered in this study, as an alternative to the potential NF plant. With the relevant chromium concentration (23 $\mu\text{g/L}$) and the same ion exchange resin performance, a total volume of 800 m^3 of adsorption material would be necessary to provide safe water during 10 years of operation, i.e., the lifetime of the NF plant. Given the high cost of this resin (20 €/L) the operating cost of a possible ion-exchange process would be >1.00 € for each m^3 of product water, significantly higher than the figure relative to the NF plant.

4.5 Environmental Impact Assessment of the full-scale NF plant

The results of the LCA analysis obtained for the full-scale NF plant of Figure 4 are reported in Figure 6, with endpoint indicators summarized in Figure 6a. The power supply needed to pump well water in the NF system at the desired hydraulic pressure and necessary to heat up the cleaning solutions overwhelms the other environmental burdens related to both concentrate treatment and the installation and operation of the membrane plant (i.e., building construction, membrane modules, and cleaning agents). This result is in accordance with previous studies, which underlined the need to improve the operating phases of membrane systems to achieve lower environmental impacts (Bonton et al. 2012; Hancock et al. 2012).

Similar results were obtained for the midpoint analysis; please see Figure S5 of the Supplementary Material for details on all the different midpoint burdens. Power supply represents the most impactful item on all midpoint parameters, except for freshwater and marine

eutrophication. Figure 6b-d present the absolute impact values relative to both these parameters, as well as to climate change. Due to the large amount of freshwater necessary for building construction, membrane module fabrication, and cleaning agents, freshwater eutrophication increases considerably. This result is in accordance with previous studies analysing the overall impacts of ultrafiltration plants (Giagnorio et al. 2017). When dealing with marine eutrophication, the most important factors increasing it are concentrate treatment and power supply, the latter also having the largest impact on CO₂ emissions.

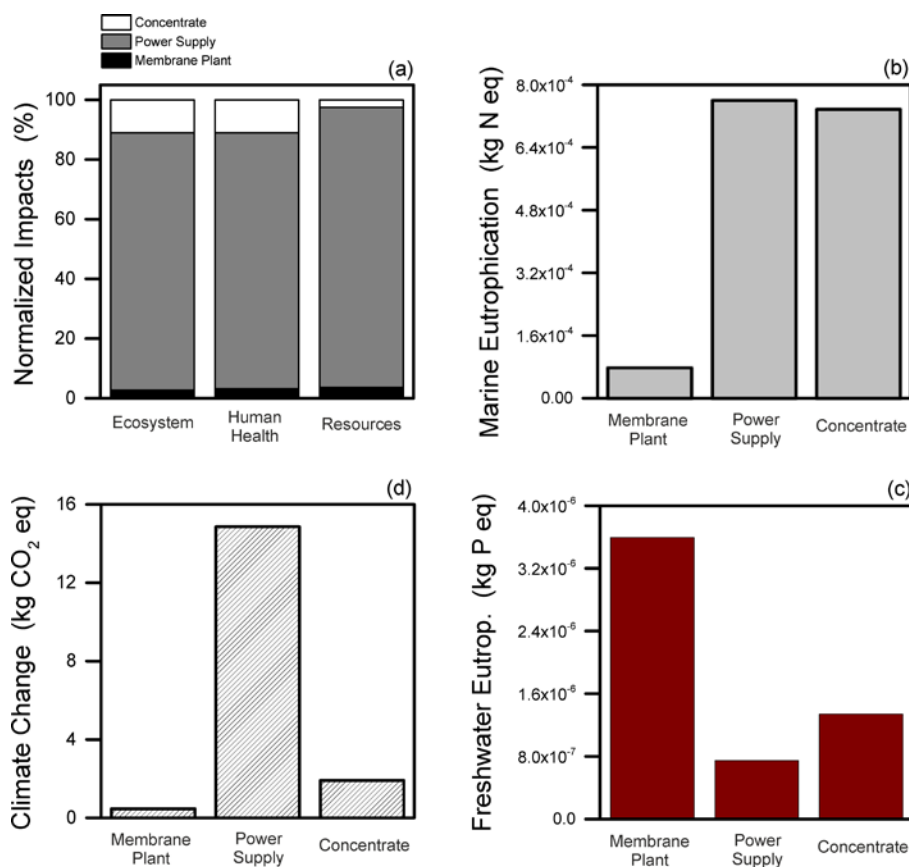


Figure 6: Environmental impacts of the full-scale NF plant. a) Results obtained through endpoint analysis, presented as normalized values of the overall impact computed for membrane plant, power demand, and concentrate treatment. b-d) Results obtained for three representative midpoint indicators.

5. Conclusions

In this paper, nanofiltration (NF) was evaluated as a potential technology to produce drinking water from sources contaminated with chromium or similar toxic metals. Through the combination of laboratory experiments, pilot-scale field tests, and system design, the applicability of NF to produce safe potable water was demonstrated. Pilot field tests suggested that low-pressure NF may be operated with minimal management issues to obtain consistently low concentrations of toxic metals in the permeate stream. Choosing the suitable nanofiltration membrane was proven to be essential to overcome inefficiencies related to fouling and to the impairment of system performance during operation. For the specific location investigated in this study, the utilization of NF membranes with medium-high selectivity was indispensable to meet the requirements in terms of drinking water quality and, specifically, of chromium concentration.

A potential design of a full-scale NF plant for chromium removal was presented, based on the specific data of the studied location, i.e., flow rate and chromium concentration in the feed stream. Two stages and a feed bypass of roughly 15% would allow the production of safe potable water with (i) an aggressive index higher than 10 and (ii) a chromium concentration lower than 5 $\mu\text{g/L}$. This design may be generalized for plants of similar size and can be used as a preliminary estimation of the plant requirements for a variety of NF applications. This generalization may be carried out also thanks to a proposed system scale analysis, which can provide preliminary guidelines for the design of generic nanofiltration systems. Specifically, at high recovery rates, the main design parameter of NF plants treating waters contaminated with toxic metals may be the composition of the final retentate stream, which needs proper management due to the resulting high concentration levels of the target toxic metal. Techno-economic and environmental assessments were performed for the potential full-scale plant. The results showed a total cost of $< 0.3 \text{ €m}^3$ for the product water, much lower than the cost of water for a plant comprising non-regenerable ion-exchange resins, which was estimated to be greater than 1 €m^3 due to the high cost of resin

replacement. The total installation cost for the NF plant was estimated to be 1.3 million € with concentrate disposal and energy requirement representing the most expensive operating parameters. Power supply would also be the most environmentally impactful factor, based on the LCA analysis performed for the installation and ten-year operation of the NF plant.

Acknowledgments

This study was supported by SMAT SpA, Società Metropolitana Acque Torino. We acknowledge Valentina Quaranta and Elena Dalla Vecchia, who assisted in the proofreading and language editing of the manuscript.

References

- Al-Rashdi BAM, Johnson DJ, Hilal N (2013) Removal of heavy metal ions by nanofiltration. *Desalination* 315: 2-17. <https://doi.org/10.1016/j.desal.2012.05.022>
- Andrade LH, Aguiar AO, Pires WL, Grossi LB, Amaral MCS (2017) Comprehensive bench-and pilot-scale investigation of NF for gold mining effluent treatment: Membrane performance and fouling control strategies. *Sep Purif Technol* 174: 44-56. <https://doi.org/10.1016/j.seppur.2016.09.048>
- Baker RW (2012): Overview of membrane science and technology. In: *Membrane Technology and Applications*, 1-14 pp
- Bannoud AH (2001) Elimination of hardness and sulfate content in water by nanofiltration. *Desalination* 137: 133-139. [https://doi.org/10.1016/S0011-9164\(01\)00211-9](https://doi.org/10.1016/S0011-9164(01)00211-9)
- Bellona C, Drewes JE (2007) Viability of a low-pressure nanofilter in treating recycled water for water reuse applications: A pilot-scale study. *Water Res* 41: 3948-3958. <https://doi.org/10.1016/j.watres.2007.05.027>
- Ben Fraes N, Taha S, Dorange G (2005) Influence of the operating conditions on the elimination of zinc ions by nanofiltration. *Desalination* 185: 245-253. <https://doi.org/10.1016/j.desal.2005.02.079>
- Bonton A, Bouchard C, Barbeau B, Jedrzejak S (2012) Comparative life cycle assessment of water treatment plants. *Desalination* 284: 42-54. <https://doi.org/10.1016/j.desal.2011.08.035>
- Chon K, Cho J (2016) Fouling behavior of dissolved organic matter in nanofiltration membranes from a pilot-scale drinking water treatment plant: An autopsy study. *Chem Eng J* 295: 268-277. <https://doi.org/10.1016/j.cej.2016.03.057>
- Costa AR, de Pinho MN (2006) Performance and cost estimation of nanofiltration for surface water treatment in drinking water production. *Desalination* 196: 55-65. <https://doi.org/10.1016/j.desal.2005.08.030>
- The Council of the European Union Council Directive 98/83/EC of 3 November 1998.
- Epsztein R, Shaulsky E, Dizge N, Warsinger DM, Elimelech M (2018) Role of Ionic Charge Density in Donnan Exclusion of Monovalent Anions by Nanofiltration. *Environ Sci Technol* 52: 4108-4116. <https://doi.org/10.1021/acs.est.7b06400>
- Espinasse BP, Chae SR, Marconnet C, Coulombel C, Mizutani C, Djafer M, Heim V, Wiesner MR (2012) Comparison of chemical cleaning reagents and characterization of foulants of nanofiltration membranes used in surface water treatment. *Desalination* 296: 1-6. <https://doi.org/10.1016/j.desal.2012.03.016>
- Garcia-Ivars J, Martella L, Massella M, Carbonell-Alcaina C, Alcaina-Miranda MI, Iborra-Clar MI (2017) Nanofiltration as tertiary treatment method for removing trace pharmaceutically active compounds in wastewater from wastewater treatment plants. *Water Res* 125: 360-373. <https://doi.org/10.1016/j.watres.2017.08.070>
- Garcia-Vaquero N, Lee E, Castaneda RJ, Cho J, Lopez-Ramirez JA (2014) Comparison of drinking water pollutant removal using a nanofiltration pilot plant powered by renewable energy and a conventional treatment facility. *Desalination* 347: 94-102. <https://doi.org/10.1016/j.desal.2014.05.036>
- Giagnorio M, Amelio A, Gruttner H, Tiraferri A (2017) Environmental impacts of detergents and benefits of their recovery in the laundering industry. *J Clean Prod* 154: 593-601. <https://doi.org/10.1016/j.jclepro.2017.04.012>
- Giagnorio M, Ruffino B, Grinic D, Steffenino S, Meucci L, Zanetti MC, Tiraferri A (2018) Achieving Low Concentrations of Chromium in Drinking Water by Nanofiltration: Membrane Performance and Selection. *Environ Sci Pollut Res*. <https://doi.org/10.1007/s11356-018-2627-5>
- World Health Organization, Guidelines for drinking-water quality. 978 92 4 154815 1, Malta
- Hancock NT, Black ND, Cath TY (2012) A comparative life cycle assessment of hybrid osmotic dilution desalination and established seawater desalination and wastewater reclamation processes. *Water Res* 46: 1145-1154. <https://doi.org/10.1016/j.watres.2011.12.004>

- Hilal N, Al-Zoubi H, Darwish NA, Mohammad AW, Abu Arabi M (2004) A comprehensive review of nanofiltration membranes: Treatment, pretreatment, modelling, and atomic force microscopy. *Desalination* 170: 281-308. <https://doi.org/10.1016/j.desal.2004.01.007>
- Hilal N, Kim GJ, Somerfield C (2011) Boron removal from saline water: A comprehensive review. *Desalination* 273: 23-35. <https://doi.org/10.1016/j.desal.2010.05.012>
- Kosutic K, Novak I, Sipos L, Kunst B (2004) Removal of sulfates and other inorganics from potable water by nanofiltration membranes of characterized porosity. *Sep Purif Technol* 37: 177-185. [https://doi.org/10.1016/S1383-5866\(03\)00206-5](https://doi.org/10.1016/S1383-5866(03)00206-5)
- Kurt E, Koseoglu-Imer DY, Dizge N, Chellam S, Koyuncu I (2012) Pilot-scale evaluation of nanofiltration and reverse osmosis for process reuse of segregated textile dyewash wastewater. *Desalination* 302: 24-32. <https://doi.org/10.1016/j.desal.2012.05.019>
- Italian Republic, Legislative Decree 2 February 2001, n. 31. Rome, Italy
- Lin JY, Tang CYY, Ye WY, Sun SP, Hamdan SH, Volodin A, Van Haesendonck C, Sotto A, Luis P, Van der Bruggen B (2015) Unraveling flux behavior of superhydrophilic loose nanofiltration membranes during textile wastewater treatment. *J Membrane Sci* 493: 690-702. <https://doi.org/10.1016/j.memsci.2015.07.018>
- Lopes MP, Matos CT, Pereira VJ, Benoliel MJ, Valerio ME, Bucha LB, Rodrigues A, Penetra AI, Ferreira E, Cardoso VV, Reis MAM, Crespo JG (2013) Production of drinking water using a multi-barrier approach integrating nanofiltration: A pilot scale study. *Sep Purif Technol* 119: 112-122. <https://doi.org/10.1016/j.seppur.2013.09.002>
- Luo YL, Guo WS, Ngo HH, Nghiem LD, Hai FI, Zhang J, Liang S, Wang XCC (2014) A review on the occurrence of micropollutants in the aquatic environment and their fate and removal during wastewater treatment. *Sci Total Environ* 473: 619-641. <https://doi.org/10.1016/j.scitotenv.2013.12.065>
- Mikulasek P, Cuhorka J (2016) Removal of Heavy Metal Ions from Aqueous Solutions by Nanofiltration. *Chem Engineer Trans* 47: 379-384. <https://doi.org/10.3303/Cet1647064>
- Minella M, De Bellis N, Gallo A, Giagnorio M, Minero C, Bertinetti S, Sethi R, Tiraferri A, Vione D (2018): Coupling of nanofiltration and thermal Fenton reaction for the abatement of carbamazepine in wastewater
- Mohammad AW, Teow YH, Ang WL, Chung YT, Oatley-Radcliffe DL, Hilal N (2015) Nanofiltration membranes review: Recent advances and future prospects. *Desalination* 356: 226-254. <https://doi.org/10.1016/j.desal.2014.10.043>
- Ong YK, Li FY, Sun SP, Zhao BW, Liang CZ, Chung TS (2014) Nanofiltration hollow fiber membranes for textile wastewater treatment: Lab-scale and pilot-scale studies. *Chem Eng Sci* 114: 51-57. <https://doi.org/10.1016/j.ces.2014.04.007>
- Radjenovic J, Petrovic M, Ventura F, Barcelo D (2008) Rejection of pharmaceuticals in nanofiltration and reverse osmosis membrane drinking water treatment. *Water Res* 42: 3601-3610. <https://doi.org/10.1016/j.watres.2008.05.020>
- Richards LA, Vuachere M, Schafer AI (2010) Impact of pH on the removal of fluoride, nitrate and boron by nanofiltration/reverse osmosis. *Desalination* 261: 331-337. <https://doi.org/10.1016/j.desa1.2010.06.025>
- Saitua H, Gil R, Padilla AP (2011) Experimental investigation on arsenic removal with a nanofiltration pilot plant from naturally contaminated groundwater. *Desalination* 274: 1-6. <https://doi.org/10.1016/j.desal.2011.02.044>
- Samhaber WM, Nguyen MT (2014) Applicability and costs of nanofiltration in combination with photocatalysis for the treatment of dye house effluents. *Beilstein J Nanotech* 5: 476-484. <https://doi.org/10.3762/bjnano.5.55>
- Sarkar B, Venkateswralu N, Rao RN, Bhattacharjee C, Kale V (2007) Treatment of pesticide contaminated surface water for production of potable water by a coagulation-adsorption-nanofiltration approach. *Desalination* 212: 129-140. <https://doi.org/10.1016/j.desal.2006.09.021>
- Schafer AI, Fane AG, Waite TD (2001) Cost factors and chemical pretreatment effects in the membrane filtration of waters containing natural organic matter. *Water Res* 35: 1509-1517. [https://doi.org/10.1016/S0043-1354\(00\)00418-8](https://doi.org/10.1016/S0043-1354(00)00418-8)

- Semiao AJC, Schafer A (2013) Removal of adsorbing estrogenic micropollutants by nanofiltration membranes. Part A-Experimental evidence. *J Membrane Sci* 431: 244-256. <https://doi.org/10.1016/j.memsci.2012.11.080>
- Taheran M, Brar SK, Verma M, Surampalli RY, Zhang TC, Valero JR (2016) Membrane processes for removal of pharmaceutically active compounds (PhACs) from water and wastewaters. *Sci Total Environ* 547: 60-77. <https://doi.org/10.1016/j.scitotenv.2015.12.139>
- Van der Bruggen B, Vandecasteele C (2003) Removal of pollutants from surface water and groundwater by nanofiltration: overview of possible applications in the drinking water industry. *Environ Pollut* 122: 435-445. [https://doi.org/10.1016/S0269-7491\(02\)00308-1](https://doi.org/10.1016/S0269-7491(02)00308-1)
- Vince F, Aoustin E, Breant P, Marechal F (2008) LCA tool for the environmental evaluation of potable water production. *Desalination* 220: 37-56. <https://doi.org/10.1016/j.desal.2007.01.021>
- Vrijenhoek EM, Hong S, Elimelech M (2001) Influence of membrane surface properties on initial rate of colloidal fouling of reverse osmosis and nanofiltration membranes. *J Membrane Sci* 188: 115-128. [https://doi.org/10.1016/S0376-7388\(01\)00376-3](https://doi.org/10.1016/S0376-7388(01)00376-3)
- Wadekar SS, Hayes T, Lokare OR, Mittal D, Vidic RD (2017) Laboratory and Pilot-Scale Nanofiltration Treatment of Abandoned Mine Drainage for the Recovery of Products Suitable for Industrial Reuse. *Ind Eng Chem Res* 56: 7355-7364. <https://doi.org/10.1021/acs.iecr.7b01329>
- Autorità d'Ambito Torinese 3, Water Management Tariffs. ARTICOLAZIONE TARIFFARIA PER IL SERVIZIO IDRICO INTEGRATO DAL 01/01/2018 FINO ALL'AGGIORNAMENTO BIENNALE DELLE TARIFFE DELIBERAZIONE AEEGSI N. 918/2017/R/IDR DEL 27/12/2017, Turin, Italy